Part One
Preparation of Nanocatalysts and Their Potential in Catalysis

1
Liquid-Phase Synthesis of Nanocatalysts

Jean-Francois Hochepied[1,2]

[1]MINES ParisTech, Centre des Matériaux, CNRS UMR 7633, BP 87 91003 Evry cedex, France
[2]ENSTA ParisTech, Unité Chimie et Procédés, 828 Bd des Maréchaux, 91762 Palaiseau cedex, France

1.1
Introduction

The control of catalysts structure at the nanoscale is the key to increase performances and improve the fundamental knowledge about reaction mechanisms. Thanks to powerful nanocharacterization tools, especially high-resolution transmission electron microscopy [1], chemists can check their ability to control critical parameters as particle size, composition, shape, exposed crystalline faces, and particle–support interfaces. This has boosted studies linking processes, nanostructures, catalytic properties measurements, and modelization, paving the way for the rational design of nanocatalysts.

Liquid-phase processes offer a compromise between industrial constraints and fine control of nanostructures. It is impossible to encompass in a few pages all processes and materials relevant to catalysts and many are considered with more details elsewhere in this book, so the point of view is to focus on two families of materials – metallic oxides and metals – and show by selected examples how they can be shaped and interfaced at the nanoscale using simple and industrially relevant processes to create nanocatalysts. In the case of oxides – either catalysts or catalysts supports – we will consider both particles and porous structures, whereas we will rather focus on particles in the case of metals, considering they can be either colloidal catalysts or supported by oxides.

Liquid-phase syntheses are bottom-up approaches consisting in condensing soluble species. The formation of solid can be described in terms of nucleation and growth (eventually followed by agglomeration) and basic theories and concepts help to understand the strategies relevant to catalysts design.

Roughly, two key parameters, supersaturation S and solid surface tension γ (or free energy), are sufficient to provide expressions for homogeneous nucleation and growth rates in solution. Surface tension is related to the energy needed to

create interfaces. In the case of a liquid (drop model), the surface chemical potential of a droplet with radius r is given by the following equation:

$$\mu_{(S,r)} = \mu_{(S,\infty)} + \frac{(2\gamma V_m)}{r},$$

where V_m is the molar volume of the condensing molecule. Similar expressions can be obtained with solids, keeping in mind that surface tension is no more isotropic if they are crystallized but depends on the exposed faces. In any case, the important point is the γ/r dependence law. Supersaturation may be defined as the ratio between the actual quotient of the reaction in solution and the equilibrium constant, and gives the driving force of precipitation. In addition, in nucleation an additional free energy term comes from the creation of a solid surface, so the expression of the free enthalpy ΔG_i for the condensation of i soluble units A into a cluster A_i can be written as follows:

$$\Delta G_i = RT\left(-i\ln(S) + \Theta i^{2/3}\right), \quad \text{with} \quad \Theta = \gamma s/(RT),$$

where s is the surface covered by one unit. Here a simplified approach considers a critical germ $i*$ defined by the maximum of ΔG_i and derive a kinetics expression for the nucleation rate J. In fact, in a more rigorous approach, the thermodynamical system with all population from $i=1$ to $i=N_{max}$ should be considered [2], but the derived expression for nucleation kinetics is the same as in the simplified approach. The critical germ can be considered as the smallest possible solid particle; in theory, it practically does not exist in solution, but its formation is the kinetics bottleneck. So in this approach, the nucleation rate J, that is, the number of germs produced per second and per volume unit, is as follows:

$$J = J_0 \exp\left(-\frac{4\Theta^3}{27(\ln S)^2}\right).$$

The expression is simple, but unfortunately supersaturation and surface tension are in general not easy to determine. If mixing of solutions is used, even with rapid mixers characteristic times for mixing are in general longer than characteristic times for nucleation. Surface tension depends on the germ facies, which is by no means similar to the equilibrium (Wulff) facies. Nevertheless, the expression gives some clues about sensitiveness of nucleation kinetics to supersaturation and surface tension. In the case of heterogeneous nucleation, a prefactor ($f<1$) is used in the expression of ΔG_i to quantify the fact that it is generally easier than homogeneous nucleation (the interfacial energy between substrate and germ is lower than between solvent and germ). It is important to keep in mind that if heterogeneous nucleation is wanted, the supersaturation must be moderate to avoid homogeneous nucleation, which explains the strategies used for controlling subtrate–nanoparticles interfaces.

If we consider the evolution of a crystalline germ, crystal growth depends on the nature of the faces. If we consider perpendicular growth (addition of new

layers on faces), high-energy faces grow faster than low-energy faces, because they can grow by continuous incorporation of matter from the solution, whereas low-energy faces grow by 2D nucleation. So the surface proportion of high-energy faces tends to lower during crystal growth. Trying to modify the relative growth rates of different faces is the basis of kinetic facies tuning. In order to tune the facies of nanoparticles, several strategies are possible. Some recipes produce germs with well-defined facets, additives that will selectively "poison" some surfaces and prevent their growth are also known more or less empirically. If we consider general expressions, nucleation, especially when initial supersaturation is very high, can consume the main part of reactants and only a small fraction can remain available for growth. This seems favorable if one just wants to synthesize nanoparticles, but a problem is the first precipitate may frequently be metastable (according to the Ostwald rule of stages [3], less stable products are kinetically favored), transforming into the stable product via redissolution under conditions of much lower supersaturation, hence more favorable to growth. It is also important to keep in mind that even when there is no more average supersaturation after precipitation, nanoparticles may still evolve due to size polydispersity: Small particles are more soluble than bigger ones due to the $1/r$ dependence law of their surface chemical potential; hence, in a medium supposed to be at the solubility "equilibrium," the average solubility level is in fact undersaturated for small particles that tend to dissolve, whereas supersaturated for big particles that tend to grow: This phenomenon is known as Ostwald ripening [4]. The same applies for facies: The chemical potential of high-energy faces is higher than that of low-energy faces, and the facies tends to change in favor of low-energy faces. Uncontrolled ripening is therefore in general detrimental to catalysts activity by lowering the surface area and exposing less active faces (Figure 1.1).
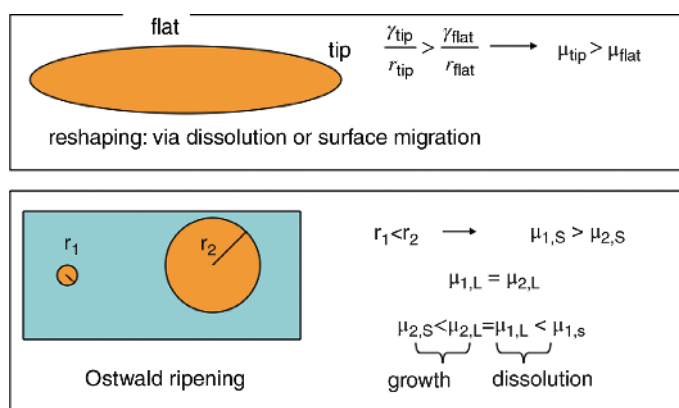
Figure 1.1 Ripening of nanoparticles in solution without apparent supersaturation. An important cause for catalysts performance loss.

1.2
Metallic Oxides

1.2.1
(Co)Precipitation by Mixing (Aqueous Solutions) and Ripening

The mixing of a concentrated aqueous solution of metallic salts and a basic solution is the most direct way to (co)precipitate metallic (hydr)oxides. The strategy is simple: generate a very high supersaturation favoring nucleation over growth, which is relatively easy when resulting (hydr)oxides are poorly soluble. In general, as precipitated products (often metastable, sometimes amorphous) need post-treatment (ripening and calcination) to be chemically and crystallographically stable, rebuild their surfaces and meet the specifications needed for the application in catalysis (Figure 1.2).

The way mixing is done is critical and can change drastically the products starting from the same solutions and considering the same final bulk conditions, as evidenced, for instance, with boehmite (mesoporous or fibrillar) precipitated by mixing aluminum nitrate with soda [5]. The most direct way of mixing two solutions consists in the injection of the basic solution into a batch containing the metallic acidic solution, but even with performant mixers the physicochemical conditions (pH, concentrations, and consequently supersaturation) of the bulk and locally at the injection point vary from the beginning to the end of the injection (even if rapid), with the risk that corresponding precipitated particles may be different. To circumvent this, in order to stabilize the physicochemical conditions in the mixing zones, a separated double-jet system is appropriate, as evidenced, for instance, for nickel hydroxide precipitation where the bulk pH was shown to control particle size and crystallinity [6]. The extreme case of double-jet consists in rapid (static) (micro)mixers, where both fluids are injected and mixed in a confined volume. The design of microreactors at various scales (from laboratory-scale
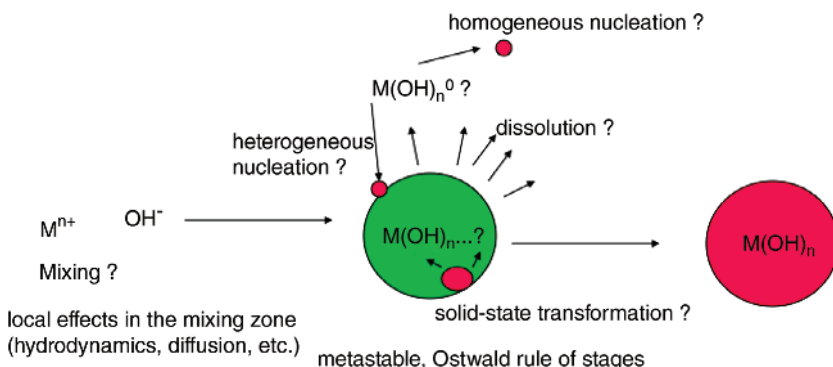

Figure 1.2 From soluble species to solid (hydr)oxides: the frequent occurrence of intermediate metastable solid (in green) must be considered in the size and shape control of final particles (in red).
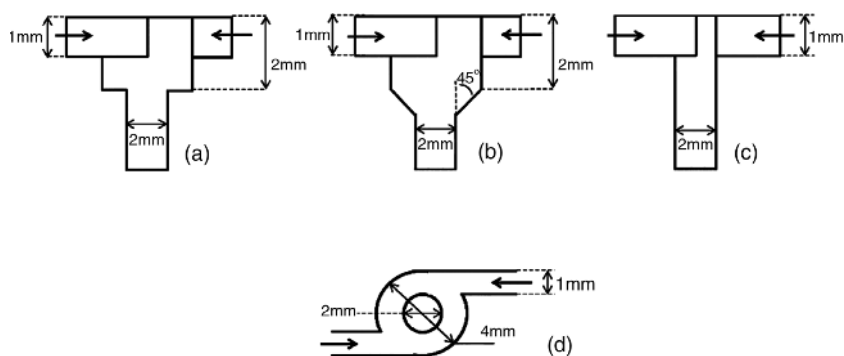
Figure 1.3 Example of geometries of Hartridge–Roughton (vortex) micromixers. (Reproduced with permission from Ref. [7]. Copyright 2016, Elsevier.)

microfluidics to industrial mixers) has been recently boosted by the increasing computing power for hydrodynamic modelization and improvements of fabrication techniques allowing precise control of device dimensions (channels, cavities) and interface quality (Figure 1.3) [7]. These continuous systems are the cornerstones of process intensification in precipitation [8]. For instance, Fang *et al.* [9] coprecipitated Fe(II) and Fe(III) to produce magnetite nanoparticles and evidenced that their rapid mixer (impinging jets) led to good crystallinity and homogeneity, Palanisamy and Paul [10] precipitated ceria continuously in a T-mixer and linked particle characteristics (homogeneity, size distribution, agglomeration) to the quality of mixing (engulfment flow conditions).

Considering aqueous solutions, in general mixing is performed under atmospheric pressure and consequently at moderate temperatures. Some batch systems (autoclaves) allow mixing under pressure in hydrothermal conditions, but most of the time mixing and hydrothermal ripening are separated steps. This may appear as a constraint, but also offers a lever to tune the product characteristics by choosing independently the physicochemical conditions for each step. The way precipitates are heated up to hydrothermal ripening is critical and some products may be sensitive to the ramp used because they can begin to transform before reaching the desired temperature, so there is a specific interest in controlling the temperature ramp accurately and if possible in reaching high heating rates. For batch systems, heating by the walls is less appropriate if fast heating is wanted, microwave heating is much more relevant but limited to relatively small volumes and as a consequence not well spread at industrial scale. Continuous systems allow fast heating even using classical transfer by the walls if exchange surfaces are high enough. In such systems, a precipitate of amorphous titanium hydroxide can be transformed into well-crystallized and well-dispersed anatase nanoparticles (10 nm) at relatively low temperature (120 °C) in a few minutes [11]. An important variation is the continuous supercritical hydrothermal synthesis (in general 400–500 °C, 30 MPa). Aimable *et al.* [12] precipitated in a few seconds nanocrystallized particles (or agglomerates) of ZrO_2,
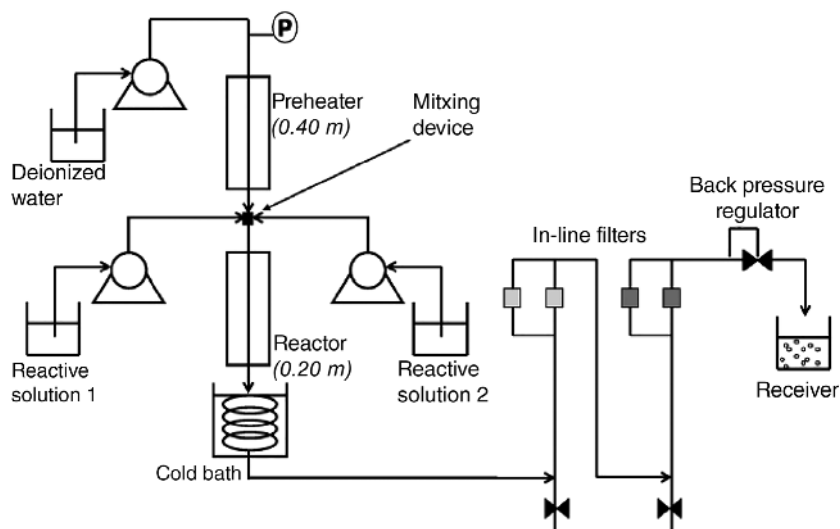
Figure 1.4 A typical equipment coupling micromixer and continuous hydrothermal ripening. (Reproduced with permission from Ref. [12]. Copyright 2009, Elsevier.)

TiO$_2$, ferrites, and perovskites in their system combining a T-mixer and a continuous flow reactor (cf. Figure 1.4). Similarly, Kawasaki *et al.* [13] produced with very short residence time (order of magnitude 1 s) well-crystallized TiO$_2$ anatase nanoparticles (in the range of 13–30 nm). It is noteworthy that these authors also used micromixers to mix the Ti(IV) solution with supercritical KOH solution to improve the control of nucleation.

Catalysts or catalyst supports are often solid solutions or doped oxides. Mixed oxides where cations have close hydrolysis reactivity can be obtained by aqueous coprecipitation. Cationic doping is sometimes more difficult when the dopant has a very different solubility compared to the cation(s) of the host matrix. If some cations are highly soluble in water (mainly from columns 1 and 2 of the classification), different strategies should be used. A cheap and convenient way consists in coprecipitating poorly soluble species as citrates, acetates, and so on if column 2 elements are involved, but particle size control is generally poor and calcination is necessary to get the oxide phase.

The advantages of aqueous (co)precipitation are obvious: Huge quantities of particles with high yields may be produced (generally >10% in mass), which is industrially relevant, in general a good average composition control can be achieved, and satisfactory crystallinity and specific surface area values may be obtained for most oxide materials (especially for tri- or tetravalent metallic cations) after appropriate posttreatments. The control of reactor geometry, propellers, and so on ensures the robustness of the process. Nevertheless, this strategy implies limitations: In general, no fine control of crystallite facies or particle size
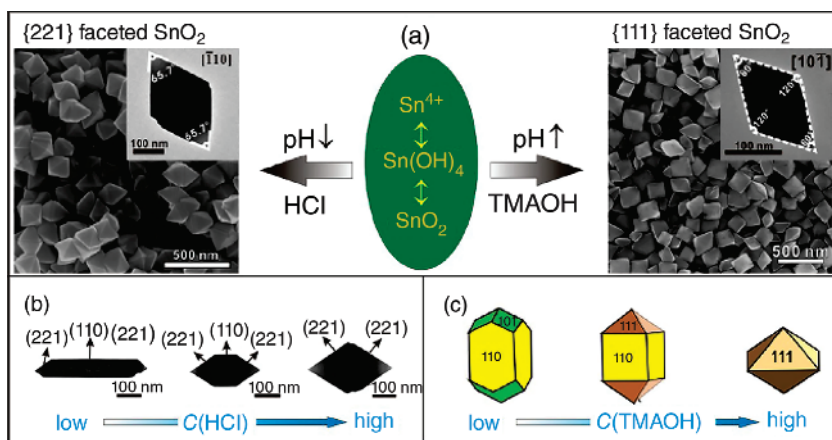
Figure 1.5 Example of pH-controlled facies of submicrometer particles. (Reproduced with permission from Ref. [14]. Copyright 2012, John Wiley & Sons, Inc.)

and shape is obtained just after precipitation and ripening conditions cannot always offer levers to change the facies in a favorable way (this depends on the mechanisms involved in the solid transformations), precipitates and powders may be strongly agglomerated, which may hinder their use.
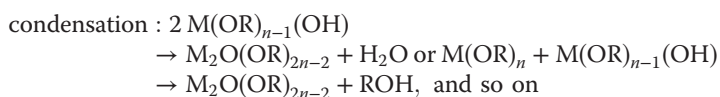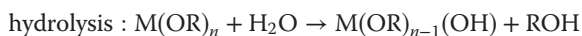
Facies or shape control may be obtained during ripening, along with crystal growth. Of course, equilibrium facies will be naturally favored, but some additives may adsorb specifically on certain faces and poison their growth. Facies is also pH dependent, since the charge of oxide faces is pH dependent, which in turn changes the surface tension. Just to give one example, Wang *et al.* [14] obtained a nice kinetic-controlled facies for SnO_2 particles just by tuning pH and studied the impact of high-energy faces exposition to promote catalytic properties (Figure 1.5).

It is also important to keep in mind that at the nanoscale, some nano-objects do not result from classical crystal growth but from other mechanisms (self-rolling of nanosheets in the case of titanate nanotubes [15], etc.).

1.2.2
Hydrolytic Sol–Gel

In classical sol–gel, a metallic alkoxide is mixed with water in alcohol. The hydrolysis of the precursor (the replacement of at least one ligand by one hydroxyl) is the first step and allow further condensation to get an oxide at the end of polymerization:

$$\text{hydrolysis}: M(OR)_n + H_2O \rightarrow M(OR)_{n-1}(OH) + ROH$$

$$\text{condensation}: 2\,M(OR)_{n-1}(OH)$$
$$\rightarrow M_2O(OR)_{2n-2} + H_2O \text{ or } M(OR)_n + M(OR)_{n-1}(OH)$$
$$\rightarrow M_2O(OR)_{2n-2} + ROH, \text{ and so on}$$

The control of the balance between the kinetics of precursor hydrolysis and condensation is the key to control the particle size and their agglomeration (formation of a gel by collisions and attachment of reactive particles). This can be achieved by the choice of the ligand, the base/acid concentration (catalyst), the choice of the alcohol, and the water/alcohol ratio. The most common precursors are Si or Ti alkoxides, and the synthesis of TiO_2 nanoparticles, nanocoatings, or nanostructures by sol–gel has been thoroughly studied. Of course, previous considerations about mixing are still valid, and the control of TiO_2 gel formation by rapid Vortex mixers was carefully studied by Marchisio *et al.* [16]. In such systems, the alkoxides of cations difficult to coprecipitate in water have very often close reactivity and copolymerize. Classical sol–gel methods lead in general to amorphous nano-oxide particles with a few nanometers in diameter, and connected by necks. Depending on the way solvent is removed, one can get nanoparticles, xerogels, or aerogels. Aerogels are obtained by CO_2 supercritical drying, keeping the integrity of the nanostructure built in solution, whereas xerogels are much denser and result from classical drying where capillary forces make the nanoarchitecture collapse. Highly porous metallic oxide aerogels offer interesting nanostructures for catalysis [17], the drawbacks being the cost of the process and their brittleness, which probably explain other families of porous materials that are nowadays hotter topics as shown elsewhere in this book. Sol–gel systems are also compatible with soft or hard templates to make ordered or hierarchical porous materials.

1.2.3
Homogeneous (Co)Precipitation by Thermohydrolysis (Aqueous Solutions)

Nanostructured microparticles may spontaneously result from homogeneous (co)precipitation in aqueous solutions, when supersaturation is generated relatively slowly (compared to mixing) in the whole volume of a solution. Generally, the precipitation is triggered by heating (using conventional or microwave sources), with different possible effects such as lowering the solubility of cations in acidic conditions (forced hydrolysis), generating a base by *in situ* decomposition (urea as main example), and removing ligands that stabilized the cations (ammonia for instance). Forced acidic hydrolysis is relevant to poorly soluble cations (Ti^{4+}, Fe^{3+}, etc.), ammonia removal to divalent transition elements (Ni^{2+}, etc.) [18], and urea decomposition to cations that can be solubilized in the initial weakly acidic conditions (Mg^{2+}, Y^{3+}, Ni^{2+}, etc.) [19]. The products may be hydroxides or hydroxycarbonates and their nanostructure may be kept when calcined to oxides. If some nanostructured multiscale particles sometimes spontaneously appear without template agents, homogeneous precipitation can be performed with hard or soft templates to generate nanoarchitectures, with possible hierarchical porosity considered as beneficial to control the diffusion of species toward catalytic surfaces. The most usual hard templates are colloidal crystals of silica or polymer spheres, and soft templates are mesophases of surfactants such as CTAB, SDS, and so on, especially used for their hexagonal

phases. After precipitation and calcination, resulting oxide architectures may exhibit both meso- and macroporosity and be optimal catalyst supports as shown by Zhou *et al.* [20] with Pd/Al_2O_3 for the selective hydrogenation of pyrolysis gasoline. Template removal (by calcination or dissolution) is often delicate and the desired porous structures may collapse during this operation.

1.2.4
Homogeneous (Co)Precipitation and/or Ripening in Nonaqueous Solvents

Aqueous-based syntheses often face two main problems: (i) Some mixed oxide materials are difficult to obtain by coprecipitation due to the difference in solubility and reactivity of metallic precursors (cations). (ii) Hydrothermal conditions, often necessary to obtain well-crystallized catalysts, require equipment working under pressure and the consequent technological, safety, and economical impacts may be heavy. Nonaqueous solvents may circumvent both issues. Solvothermal crystallization is often possible under atmospheric pressure (up to reflux) or at least under lower autogenous pressures compared to water, but of course chemistry must be adapted by choosing or synthesizing appropriate precursors in terms of solubility and reactivity. In general, the precursors decompose thermally, while the solvent and/or additives limit and/or orient particle growth after nucleation. These processes are often better than aqueous syntheses for controlling the size, composition, crystallinity, crystal habit, and architectures of particles, especially at the nanoscale, but their economical and environmental costs are higher. Production of oxides in polyols generally uses water as reagent, but in other non-aqueous systems metallic oxides can be produced using an organic molecule instead of water as the source molecule for oxygen atoms: for instance, alkoxides or ethers with metallic chloride precursors dissolved in CH_2Cl_2 [21], benzylalcohol [22], or even a polyol [23] also playing the role of solvent. This nonhydrolytic sol–gel is interesting to produce well-crystallized nanoparticles and mixed oxides. If research works seem more focused on nanoparticles, some studies show that these routes are also interesting for textured or porous materials without need for templates nor supercritical drying [21].

1.2.5
Anodization

Anodization of some metallic foils may spontaneously lead to nanostructured oxide surfaces. As main examples relevant to catalysis, we may cite alumina porous membranes and titania nanotube arrays, which have drawn a lot of attention in the field of photocatalysis [24]. The setup is simple, and the concentration of the electrolytes, pH, and anodization potential control the formation of arrays [24]. For instance, TiO_2 nanotubes arrays in Figure 1.6 were produced by anodic oxidation at a potential of 25 V of a Ti foil in a KF electrolyte at pH 4, during 17 h.
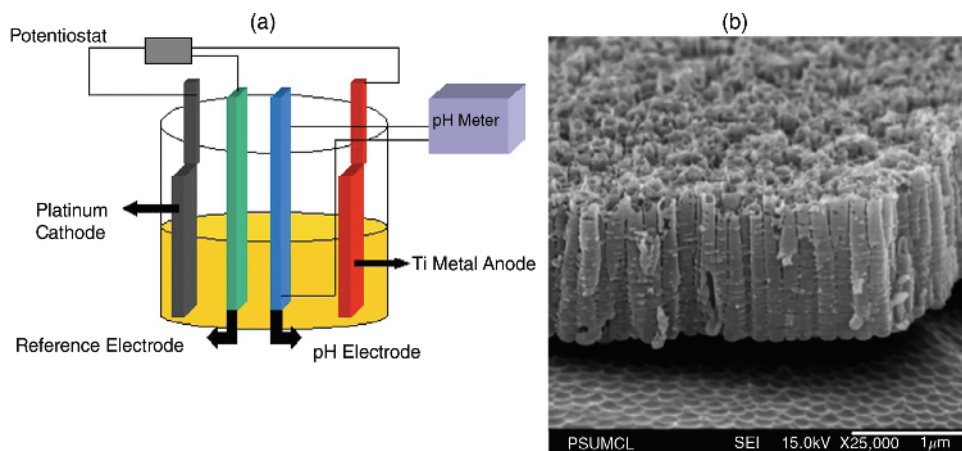
Figure 1.6 Anodization setup (a) and TiO$_2$ nanotubes arrays produced by this technique (b). (Reproduced with permission from Ref. [24]. Copyright 2006, Elsevier.)

1.3
Metallic Nanoparticles

The size reduction of metallic particles to the nanolevel induces geometrical and electronic effects, both playing a role in their catalytic properties (activity and selectivity). Well-faceted polyhedral metallic nanoparticles have a significant fraction of atoms not only on crystal faces but also on edges or even corners, sites that are likely favorable to high catalytic activity. In addition, some high-index faces may exhibit steps and kinks as active sites for catalytic reactions. Syntheses allowing size, shape, and facies control of very small NP (<10 nm) are consequently highly valuable for fundamental understanding and applications. Nevertheless, a disturbing feature is that very small NPs exposing high-energy faces are thermodynamically unstable, which means their facies may undergo some evolution detrimental to performances. In some conditions used for catalytic reactions, Ostwald ripening can lead to both size increase and shape transformation into more stable (and much less catalytic) particles so quickly that studies about optimizing the facies could be considered as vain. For instance, the transformation of tetrahedral Pd particle into spherical ones was already observed after the first cycle of the Suzuki reactions [25]. The stabilization of metallic NPs (against ripening or irreversible aggregation in liquid media) with organic molecules is possible, but their surface modification changes their catalytic behavior. Fortunately enough, if in general they lower the catalytic activity on the one hand, capping agents may promote selectivity as underlined in Ref. [26] on the other hand. As far as solvents are concerned, most of metallic nanoparticles relevant to catalysis can be obtained in aqueous systems. An industrially acceptable alternative is offered by polyol-mediated syntheses. Other nonaqueous systems may give better control on particle dimensions at the

nanolevel, but are not industrially well spread and since they are less useful in the field of catalysis compared to other applications, they will not be considered here.

1.3.1
Aqueous Syntheses

Some metallic nanoparticles can be produced by adding hydrides to metallic cations, and (as for oxide precipitation) the control of mixing is critical. Thiele *et al.* [27] have shown that well-controlled silver seeds could be obtained in their microfluidic homemade device using micromixers to mix $AgNO_3$ and $NaBH_4$ solutions (Figure 1.7). The size control is found better than obtained with a batch reactor. These seeds can be used for growing nanotriangles in a second and separated step, with precise dimensions control.

Homogeneous precipitation of metallic particles uses less reactive reductors than hydrides, and is generally activated by heating after mixing in nonreactive conditions (low temperature). For instance, a simple recipe to produce gold nanoparticles consists in dissolving $HAuCl_4$ in water, adding sodium citrate, adjusting pH to a desired value, and heating at moderate temperatures; of course, from the stem work by Turkevich [28], many studies were however necessary to describe thoroughly this system, explain the mechanisms at the basis of size and shape tuning [29].
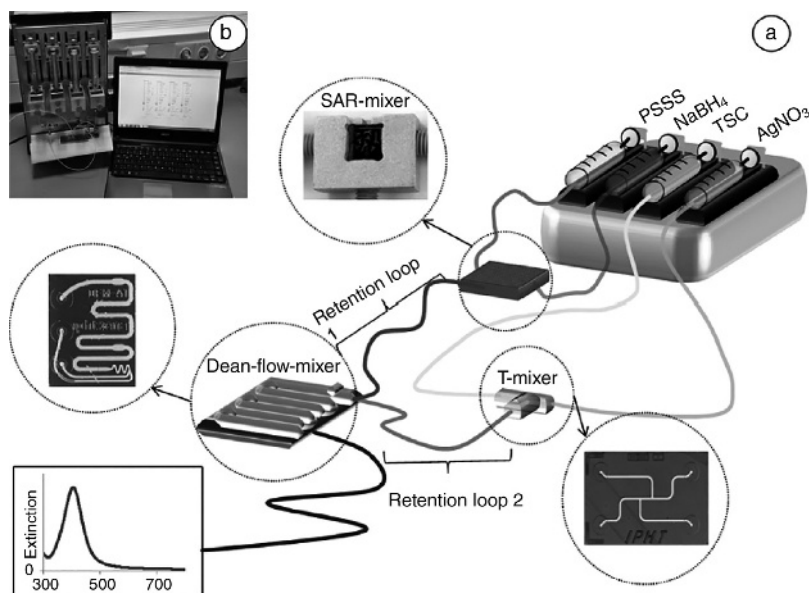
Figure 1.7 Continuous flow synthesis of silver nanoparticles using micromixers. (Reproduced with permission from Ref. [27]. Copyright 2015, John Wiley & Sons, Inc.)

Size, shape, and facies control is now mastered for many metallic NPs, often via seed-mediated growth. Well-faceted germs can be obtained by controlling nucleation conditions, and then additives as anions, metallic cations, polymers, surfactants, or other organic molecules, chosen or discovered more or less empirically, selectively adsorb on well-defined crystallographic face and impede or accelerate their growth. Of course, the downside of this method is the risk of persistence of directing agents after synthesis and the consequent alteration of the catalytic activity of the relative faces. Some articles only deal with the synthesis of particle with well-defined facets, but some study continuous shape tuning (from spherical to cubes, from cubes to octahedra, etc.), generally going along with limited growth, showing the intermediate states, which is of course of the highest interest for catalytic properties studies. For instance, CTAB preferential adsorption to (100) rather than (111) faces of gold allows kinetic shape tuning [30]. In addition to poisoning, oxidative etching, attacking preferential faces, can be used to dissolve selectively particles with specific facies [31]. As an example of shape control directly applied to catalysis, Berhault *et al.* [32] studied the effect of Pd NP shape and facies on the selective hydrogenation of buta-1,3-diene by synthesizing nanocubes, nanotetrahedra, and nanorods, thanks to a seed-mediated approach and the surfactant CTAB (easily removed after synthesis) as inhibitor of (100) facets growth. They proved that the preferential exposure of (100) planes in rods allowed a high selectivity for the conversion into butenes. At the nanoscale, one must also keep in mind that some unusual facies and shapes may be promoted compared to their bulk counterpart. For instance, seed-mediated growth approach was found very efficient to produce gold nanorods. Gold has a cubic structure, and the existence of nanorods results in fact from growth of fivefold twinned gold seed or other seeds (Pt, Ag, etc.).

1.3.2
Polyol-Mediated Syntheses

Among these systems, we may cite polyol-mediated syntheses, polyols being both reducing agents and solvents. For instance, Bonet *et al.* [33] demonstrated the relevance of polyols to produce gold, platinum, palladium, ruthenium, and iridium nanoparticles. Surfactants, capping ligands, or even well-chosen anions can be added to tune particle size and shape in the same logic as in aqueous solutions. Wiley *et al.* [34] successfully tuned the shape of Ag nanocrystals by chloride addition. Interestingly, some additives may accelerate specific face growth (instead of poisoning). Song *et al.* [35] evidenced that Ag^+ ions could promote (100) face growth in Pt nanocrystals, allowing shape tuning from cubes, cuboctahedra, and octahedra just by changing the quantity of Ag^+. Ag is first specifically reduced on (100) Pt faces, and then Ag(0) accelerates the reduction of Pt(IV) and is reoxidized and dissolved simultaneously. This process is interesting because the exposed faces do not result from poisoning, avoiding issues about possible persistent adsorption of additives. The combination of poisoning and oxidative etching gave spectacular results in polyol with fine shape tuning

for, for instance, Pd [36]. Another interesting point about polyol is their high compatibility with microwave heating.

1.3.3
Hollow Particles by Galvanic Replacement

Galvanic replacement has recently been used to produce and study hollow metallic particles and metallic nanoframes [37]. A metallic nanoparticle (often Ag, easy to oxidize) playing the role of a sacrificial template is oxidized (generally in aqueous solutions) by a metallic cation that is reduced on the surface: Au, Pt, or Pd nanocages can be obtained this way, as well as alloys and shell–shell nanocages. These hollow particles and nanoframes are supposed to enhance their catalytic activity by confinement of the reactants in their cavity. Nevertheless, for the time being, such methods cannot produce significant amounts of materials, consume relatively expensive templates, and as a consequence are still industrially irrelevant.

1.4
Oxide–Metal Interfaces

Nowadays, the variety of synthetic methods, the availability of characterization techniques at the nanoscale [38], and the increasing modelization of heterogeneous catalysis open the way to the rational design of metal–oxide catalysts with optimization of the oxide architecture (or particle size and shape) and exposed faces, optimization of the metallic particles size and shape, and last but not least the interface between metallic NP and the oxide support. See, for example, the case of CeO_2/Au nanocatalysts in Ref. [39].

An important point is that the oxide is often more than a support and can be a catalyst itself as with TiO_2 photocatalysts. So the oxide material can be a porous structure, a microparticle, or a nanoparticle, and the catalyst is in fact a hybrid (or heterostructure) between the oxide and the metal, where the nature of the junction (coherent interface or not) may play a key role in electron transfers and consequently catalytic activity. In the case of oxide semiconductor photocatalysts, the photoelectron migration to the metallic particle, preventing the recombination with the hole located in the valence band of the oxide, is assumed to be the main cause for the much higher photocatalytic activity of TiO_2 (or ZnO) when covered with metallic NP (Ag, for instance). Generally, in order to create metal–oxide hybrids, it is easier to precipitate metallic particle on oxide substrate than the opposite, with some exceptions including surface oxidation of metallic substrates.

Direct deposition of metallic NPs on oxide substrates is possible, but the nature of the interface and the dispersion is far from optimal so far as the catalytic activity and reusability are concerned. Another common approach, wet impregnation, consists in mixing noble metal soluble precursors with the

substrates, evaporating the solvent, and finally reducing in dry form by gas-phase reactions. In order to improve the control of the oxide–metal interface, a more relevant strategy is the chemisorption of metallic precursors on the surface followed by *in situ* reduction. The knowledge of the oxide surface physicochemistry (pH-dependent surface charge (zeta potential)), measured or evaluated (for instance, by multisite complexation models), guides the choice for the precursor and the best conditions to adsorb it. As an example of electrostatically favorable adsorption, ammonia can solubilize by complexation of many metallic cations (transition metals, Pt, Pd, Ru,) in basic conditions, a positively charged complex being the main species ($Pt(NH_3)_4^{2+}$, etc.), whereas oxide surfaces are negatively charged. The opposite approach, adsorbing anionic species on positively charged oxide (in acidic conditions), is of course possible and was found very relevant in the case of gold. Adsorbed species can therefore act as favored nucleation sites for further reduction and growth of metallic particles, or even be directly calcined. It is noteworthy that the reducing agent can also be the molecule complexing the metal cation. Recently, many studies compared such adsorption methods with more brutal methods as wet impregnation, and the better dispersion of NPs onto the surface and interface coherence systematically leads to better performances, as shown by Li *et al.* for Pd/TiO_2 for the Heck coupling reaction [40]. As an interesting variation, Zhong *et al.* [41] first adsorbed Sn(II) onto TiO_2 surface, which reduced Pd *in situ* to get well-dispersed Pd nanoparticles supported by TiO_2, with high loading and activity for Suzuki cross-coupling reaction. Zhang *et al.* [42] used the photocatalytic properties of TiO_2 to photodeposit Pd and evidenced the role of pH in the control of Pd particle size and dispersion. In aqueous systems, both the speciation of the metallic precursors and the surface charge of the oxide substrate are pH dependent and it is not too surprising that pH is the key physicochemical parameter when dealing with *in situ* reduction. A good knowledge of the system physicochemistry helps to control heterogeneous nucleation and growth by smooth tuning of supersaturation, avoiding shifting to homogeneous nucleation. Depending on the crystalline nature of the oxide and metal, the resulting interface may be coherent (with lattice matching), which in general changes drastically the catalytic or photocatalytic properties (electron transfer through the interface, nature of the metal–oxide medium triple line, etc.). As an example, Haruta *et al.* [43] deposited gold nanoparticles on TiO_2 (anatase) substrates by direct impregnation, resulting in ill-defined interface and precursor adsorption followed by reduction resulting in coherent interface (Figure 1.8). Propylene epoxidation was possible only with the catalyst with coherent interface, whereas the other one catalyzed only the full oxidation of the organic molecule.

Interestingly, besides NP deposition or *in situ* synthesis on preexisting surface, it is possible to synthesize the oxide matrix around metallic particles, Kónya *et al.* [44] prepared this way nanocatalysts with well-defined Pt shape in SBA-15 matrix.

One-pot synthesis of oxide matrix and metal nanoparticles with controlled oxide matrix architecture, NP particle size and shape, and metal–oxide interface
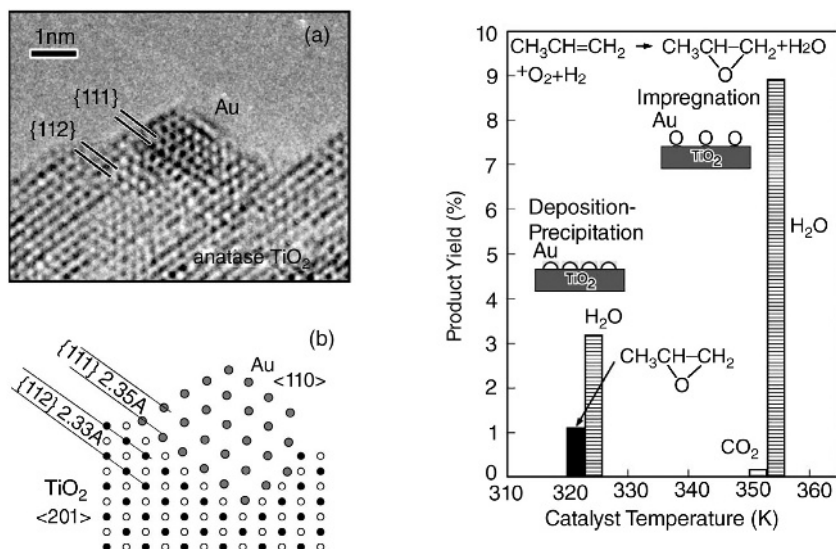
Figure 1.8 Example of process–catalytic activity relationship and interpretation by the quality of the oxide–metal interface. (From Ref. [43].)

is possible in some cases. As an example, Chen *et al.* [45] produced Pt-SBA-15 by calcining a hybrid prepared by solution chemistry: A hexagonal direct meso-phase was produced with Pt source embedded, thanks to a thiol with the templating block copolymers in the hydrophobic channels, whereas tetraethylorthosilicate TEOS polymerized in the continuous aqueous phase. Then calcination removed all organics and reduced Pt simultaneously, via decomposition of intermediate platinum sulfide. These catalysts were found better for methylcyclohexane dehydrogenation compared to conventional Pt-SiO$_2$.

1.5
Conclusion

The understanding of catalysts activity and selectivity is making continuous progress, thanks to nanocharacterization and modelization, and structure–activity (or selectivity) relationships are more and more evidenced. The rational design of new catalyst needs a trustworthy toolbox of processes allowing nano-level control of key characteristics as composition, crystallographic structure, dimensions, architectures, and interfaces. In this toolbox, liquid-phase (mainly aqueous) syntheses benefit from a rather long history in precipitation, with many thermodynamic and kinetic data available for chemical engineers. Many recipes have been optimized, and they offer other practical advantages: equipment are in general simple and affordable, process parameters are easily tunable, and continuous processes allow industrial scale-up . . . From the academic point

of view, research proved that intriguing interfacial reactivity at the nanoscale could produce original nanostructures of high interest in catalysis. Of course, a compromise must be found between industrial and environmental costs on the one hand and the performances on the other, but in any case liquid-phase syntheses are versatile enough to support both academic discoveries and industrial developments of nanocatalysts.

References

1 Akita, T., Kohyama, M., and Haruta, M. (2013) Electron microscopy study of gold nanoparticles deposited on transition metal oxides. *Acc. Chem. Res.*, **46** (8), 1773–1782.

2 Cournil, M. and Gohar, P. (1989) Thermodynamic model of supersaturated liquid solutions: application to the homogeneous nucleation of potassium sulfate. *J. Colloid Interface Sci.*, **132** (1), 188–199.

3 Nývlt, J. (1995) The Ostwald rule of stages. *Cryst. Res. Technol.*, **30** (4), 443–449.

4 (a) Kahlweit, M. (1975) Ostwald ripening of precipitates. *Adv. Colloid Interface Sci.*, **5** (1), 1–35. (b) Voorhees, P.W. (1985) The theory of Ostwald ripening. *J. Stat. Phys.*, **38** (1), 231–252.

5 Hochepied, J.F., Ilioukhina, O., and Berger, M.H. (2003) Effect of the mixing procedure on aluminium (oxide)-hydroxide obtained by precipitation of aluminium nitrate with soda. *Mater. Lett.*, **57** (19), 2817–2822.

6 Coudun, C., Grillon, F., and Hochepied, J.F. (2006) Surfactant effects on pH-controlled synthesis of nickel hydroxides. *Colloid Surf. A*, **280** (1–3), 23–31.

7 Di Patrizio, N., Bagnaro, M., Gaunand, A., Hochepied, J.-F.O., Horbez, D., and Pitiot, P. (2016) Hydrodynamics and mixing performance of Hartridge Roughton mixers: influence of the mixing chamber design. *Chem. Eng. J.*, **283**, 375–387.

8 Ghanem, A., Lemenand, T., Della Valle, D., and Peerhossaini, H. (2014) Static mixers: mechanisms, applications, and characterization methods – a review. *Chem. Eng. Res. Des.*, **92** (2), 205–228.

9 Fang, M., Ström, V., Olsson, R.T., Belova, L., and Rao, K.V. (2011) Rapid mixing: a route to synthesize magnetite nanoparticles with high moment. *Appl. Phys. Lett.*, **99** (22), 222501.

10 Tseng, C.H.T., Paul, B.K., Chang, C.-H., and Engelhard, M.H. (2013) Continuous precipitation of ceria nanoparticles from a continuous flow micromixer. *Int. J. Adv. Manuf. Technol.*, **64** (1), 579–586.

11 Malinger, K.A., Maguer, A., Thorel, A., Gaunand, A., and Hochepied, J.-F.O. (2011) Crystallization of anatase nanoparticles from amorphous precipitate by a continuous hydrothermal process. *Chem. Eng. J.*, **174** (1), 445–451.

12 Aimable, A., Muhr, H., Gentric, C., Bernard, L., Cras, F., and Aymes, D. (2009) Continuous hydrothermal synthesis of inorganic nanopowders in supercritical water: towards a better control of the process. *Powder Technol.*, **190** (1–2), 99–106.

13 Kawasaki, S.-I., Xiuyi, Y., Sue, K., Hakuta, Y., Suzuki, A., and Arai, K. (2009) Continuous supercritical hydrothermal synthesis of controlled size and highly crystalline anatase TiO$_2$ nanoparticles. *J. Supercrit. Fluids*, **50** (3), 276–282.

14 Wang, X., Han, X., Xie, S., Kuang, Q., Jiang, Y., Zhang, S., Mu, X., Chen, G., Xie, Z., and Zheng, L. (2012) Controlled synthesis and enhanced catalytic and gas-sensing properties of tin dioxide nanoparticles with exposed high-energy facets. *Chem. Eur. J.*, **18** (8), 2283–2289.

15 Kasuga, T., Hiramatsu, M., Hoson, A., Sekino, T., and Niihara, K. (1998) Formation of titanium oxide nanotube. *Langmuir*, **14** (12), 3160–3163.

16 Marchisio, D.L., Omegna, F., and Barresi, A.A. (2009) Production of TiO$_2$ nanoparticles with controlled

characteristics by means of a Vortex Reactor. *Chem. Eng. J.*, **146** (3), 456–465.

17 Schneider, M. and Baiker, A. (1997) Titania-based aerogels. *Catal. Today*, **35** (3), 339–365.

18 Coudun, C. and Hochepied, J.F. (2005) Nickel hydroxide "stacks of pancakes" obtained by the coupled effect of ammonia and template agent. *J. Phys. Chem. B*, **109**, 6069–6074.

19 Shishido, T., Yamamoto, Y., Morioka, H., and Takehira, K. (2007) Production of hydrogen from methanol over Cu/ZnO and Cu/ZnO/Al$_2$O$_3$ catalysts prepared by homogeneous precipitation: steam reforming and oxidative steam reforming. *J. Mol. Catal. A*, **268** (1–2), 185–194.

20 Zhou, Z., Zeng, T., Cheng, Z., and Yuan, W. (2011) Diffusion-enhanced hierarchically macro-mesoporous catalyst for selective hydrogenation of pyrolysis gasoline. *AIChE J.*, **57** (8), 2198–2206.

21 Debecker, D.P., Hulea, V., and Mutin, P.H. (2013) Mesoporous mixed oxide catalysts via non-hydrolytic sol–gel: a review. *Appl. Catal. A*, **451**, 192–206.

22 Niederberger, M., Bartl, M.H., and Stucky, G.D. (2002) Benzyl alcohol and titanium tetrachloride: a versatile reaction system for the nonaqueous and low-temperature preparation of crystalline and luminescent titania nanoparticles. *Chem. Mater.*, **14** (10), 4364–4370.

23 Morselli, D., Niederberger, M., Bilecka, I., and Bondioli, F. (2014) Double role of polyethylene glycol in the microwaves-assisted non-hydrolytic synthesis of nanometric TiO$_2$: oxygen source and stabilizing agent. *J. Nanopart. Res.*, **16** (10), 1–11.

24 Mor, G.K., Varghese, O.K., Paulose, M., Shankar, K., and Grimes, C.A. (2006) A review on highly ordered, vertically oriented TiO$_2$ nanotube arrays: fabrication, material properties, and solar energy applications. *Sol. Energy Mater. Sol. Cells*, **90** (14), 2011–2075.

25 Narayanan, R. and El-Sayed, M.A. (2005) Effect of colloidal nanocatalysis on the metallic nanoparticle shape: the Suzuki reaction. *Langmuir*, **21** (5), 2027–2033.

26 Niu, Z. and Li, Y. (2014) Removal and utilization of capping agents in nanocatalysis. *Chem. Mater.*, **26** (1), 72–83.

27 Thiele, M., Knauer, A., Csáki, A., Mallsch, D., Henkel, T., Köhler, J.M., and Fritzsche, W. (2015) High-throughput synthesis of uniform silver seed particles by a continuous microfluidic synthesis platform. *Chem. Eng. Technol.*, **38** (7), 1131–1137.

28 Turkevich, J., Stevenson, P.C., and Hillier, J. (1951) A study of the nucleation and growth processes in the synthesis of colloidal gold. *Discuss. Faraday Soc.*, **11** (0), 55–75.

29 (a) Gole, A. and Murphy, C.J. (2004) Seed-mediated synthesis of gold nanorods: role of the size and nature of the seed. *Chem. Mater.*, **16** (19), 3633–3640. (b) Gou, L. and Murphy, C.J. (2005) Fine-tuning the shape of gold nanorods. *Chem. Mater.*, **17** (14), 3668–3672. (c) Kimling, J., Maier, M., Okenve, B., Kotaidis, V., Ballot, H., and Plech, A. (2006) Turkevich method for gold nanoparticle synthesis revisited. *J. Phys. Chem. B*, **110** (32), 15700–15707. (d) Sau, T.K. and Murphy, C.J. (2004) Room temperature, high-yield synthesis of multiple shapes of gold nanoparticles in aqueous solution. *J. Am. Chem. Soc.*, **126** (28), 8648–8649. (e) Sau, T.K. and Murphy, C.J. (2004) Seeded high yield synthesis of short Au nanorods in aqueous solution. *Langmuir*, **20** (15), 6414–6420.

30 Nikoobakht, B. and El-Sayed, M.A. (2003) Preparation and growth mechanism of gold nanorods (NRs) using seed-mediated growth method. *Chem. Mater.*, **15** (10), 1957–1962.

31 Lim, B., Jiang, M., Tao, J., Camargo, P.H.C., Zhu, Y., and Xia, Y. (2009) Shape-controlled synthesis of Pd nanocrystals in aqueous solutions. *Adv. Funct. Mater.*, **19** (2), 189–200.

32 Berhault, G., Bisson, L., Thomazeau, C., Verdon, C., and Uzio, D. (2007) Preparation of nanostructured Pd particles using a seeding synthesis approach: application to the selective hydrogenation of buta-1,3-diene. *Appl. Catal. A*, **327** (1), 32–43.

33 Bonet, F., Tekaia-Elhsissen, K., and Sarathy, K.V. (2000) Study of interaction of ethylene glycol/PVP phase on noble

metal powders prepared by polyol process. *Bull. Mater. Sci.*, **23** (3), 165–168.

34 Wiley, B., Herricks, T., Sun, Y., and Xia, Y. (2004) Polyol synthesis of silver nanoparticles: use of chloride and oxygen to promote the formation of single-crystal, truncated cubes and tetrahedrons. *Nano Lett.*, **4** (9), 1733–1739.

35 Song, H., Kim, F., Connor, S., Somorjai, G.A., and Yang, P. (2005) Pt nanocrystals: shape control and Langmuir-Blodgett monolayer formation. *J. Phys. Chem. B*, **109** (1), 188–193.

36 Xiong, Y., Cai, H., Wiley, B.J., Wang, J., Kim, M.J., and Xia, Y. (2007) Synthesis and mechanistic study of palladium nanobars and nanorods. *J. Am. Chem. Soc.*, **129** (12), 3665–3675.

37 Fang, Z., Wang, Y., Liu, C., Chen, S., Sang, W., Wang, C., and Zeng, J. (2015) Rational design of metal nanoframes for catalysis and plasmonics. *Small*, **11** (22), 2593–2605.

38 Akita, T., Tanaka, K., Tsubota, S., and Haruta, M. (2000) Analytical high-resolution TEM study of supported gold catalysts: orientation relationship between Au particles and TiO$_2$ supports. *J. Electron Microsc.*, **49**, 657–662.

39 Ta, N., Liu, J., and Shen, W. (2013) Tuning the shape of ceria nanomaterials for catalytic applications. *Chinese J. Catal.*, **34** (5), 838–850.

40 Li, Z., Chen, J., Su, W., and Hong, M. (2010) A titania-supported highly dispersed palladium nano-catalyst generated via *in situ* reduction for efficient Heck coupling reaction. *J. Mol. Catal. A*, **328** (1–2), 93–98.

41 Zhong, L.-S., Hu, J.-S., Cui, Z.-M., Wan, L.-J., and Song, W.-G. (2007) *In-situ* loading of noble metal nanoparticles on hydroxyl-group-rich titania precursor and their catalytic applications. *Chem. Mater.*, **19** (18), 4557–4562.

42 Zhang, F., Chen, J., Zhang, X., Gao, W., Jin, R., and Guan, N. (2004) Simple and low-cost preparation method for highly dispersed Pd/TiO$_2$ catalysts. *Catal. Today*, **93–95**, 645–650.

43 (a) Haruta, M. and Daté, M. (2001) Advances in the catalysis of Au nanoparticles. *Appl. Catal. A*, **222** (1–2), 427–437. (b) Haruta, M., Uphade, B.S., Tsubota, S., and Miyamoto, A. (1998) Selective oxidation of propylene over gold deposited on titanium-based oxides. *Res. Chem. Intermed*, **24** (3), 329–336.

44 Kónya, Z., Puntes, V.F., Kiricsi, I., Zhu, J., Alivisatos, P., and Somorjai, G.A. (2002) Novel two-step synthesis of controlled size and shape platinum nanoparticles encapsulated in mesoporous silica. *Catal. Lett.*, **81** (3), 137–140.

45 Chen, A., Zhang, W., Li, X., Tan, D., Han, X., and Bao, X. (2007) One-pot encapsulation of Pt nanoparticles into the mesochannels of SBA-15 and their catalytic dehydrogenation of methylcyclohexane. *Catal. Lett.*, **119** (1), 159–164.